Anal. Methods Environ. Chem. J. 8 (1) (2025) 100-114

AMECJ

Research Article, Issue 1
Analytical Methods in Environmental Chemistry Journal
Journal home page: www.amecj.com/ir

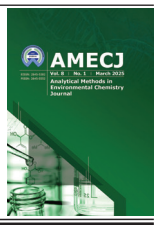

Evaluation of acridine orange dye adsorption using a new epoxy resin hardener, and degradation efficiency through the Fenton method

Saja H. Muhammed[a], Ali Abdulrazzaq Abdulwahid[a,*] and Tahseen A. Saki[a]
[a] *University of Basra, Al-Ashar–Corniche Street, postal code: 61004, Basra, Iraq*

ARTICLE INFO:
Received 25 Oct 2024
Revised form 11 Jan 2025
Accepted 14 Feb 2025
Available online 29 March 2025

Keywords:
Adsorption,
Epoxy Resin,
Fenton,
Acridine Orange,
Dye Degradation,
UV– visible spectroscopy

ABSTRACT
This research uses the Fenton process and adsorption to treat cationic Acridine Orange dye (AO) in aqueous solutions. In the Fenton method the effects of dye concentration, H_2O_2/ Fe^{2+} ratio, pH, and reaction time are considered to optimize the oxidative process. The experimental results regarding the removal percentage of AO dye are reported. UV-visible spectroscopy determined the amount of AO dye at 492nm. The optimal reaction conditions to degrade dye from aqueous solutions were: pH 4; 1.0 mM Fe^{2+} and 1.0 mM H_2O_2. On the other hand, four more robust epoxy resins, denoted E1 through E4, were synthesized using 4-aminopyridine, 3,3-diaminobenzidine (EDAB), 4-aminobenzoyl hydrazine and polyamine, and characterized using thermogravimetric analysis (TGA), and Fourier transform infrared spectroscopy (FTIR). These epoxy resins proved effective for removing AO dye from an aqueous solution at pH 10, and their adsorption behavior was in keeping with Langmuir's adsorption model. Comparison between the adsorption and photo-Fenton oxidation process for Acridine Orange (AO) was carried out under different application conditions. Epoxy resins exhibited the maximum adsorption capacity with 980.39, 1515.2, 1694.9, and 1851.9 mg g^{-1} for E1-E4 respectively at 25 °C after 1.0 h of shaking time while 81.87% of AO was utterly degraded after 10 min of photo-Fenton process.

1. Introduction

Dyes in wastewater can be harmful to people and the environment. They can be toxic, mutagenic, or carcinogenic. Water contamination is common because industries release a lot of dyes into the environment [1]. Removing dyes from wastewater is a big challenge. Many methods have been tried, including coagulation, oxidation, membrane filtration, and adsorption [2]. Adsorption stands out among these methods for removing dyes from wastewater because it's simple, easy to use, affordable, and effective. Polymeric sorbents, which can be customized in many ways and easily handle organic pollutants, are particularly promising [3]. Epoxy resins, a synthetic material, have been underused in designing adsorbents for dye removal. They're cheap, stable, and can be modified to have the right properties. While epoxy resins are increasingly used in other fields, they've seen little application in wastewater treatment. This is an area worth exploring further [4]. Epoxy resins get cross-linked when the resin reacts with a specific crosslinker's functional groups (oxirane

*Corresponding Author: Ali Abdulrazzaq Abdulwahid
Email: ali.abdulwahid@uobasrah.edu.iq
https://doi.org/10.24200/amecj.v8.i01.1013

rings). The linear resins in the curing process change into a spatially network, which makes the polymer gain many specifications such as high mechanical strength, hardness and brittleness, high chemical resistance and electrical isolation, good adhesion to metals, glass, wood and others [5]. Due to its basicity and nonhydrolyzability, ligation chemistry with low molecular weight amines such as ethylene diamine and diethylene triamine is also interesting. Consequently, it would be intriguing to create and synthesize polymeric network-type sorbents that combine the structural characteristics of amines and epoxy [6]. Recently, a novolac - based network polymer with ethylenediamine units was studied for its potential to remove azo dyes. Adding these units and using the polymer's chemical properties, a new version with diethylenetriamine sites is needed for better dye removal [7]. It would be exciting to make polymeric network sorbents that combine the best features of epoxy resins and amines. Epoxy resins are ideal because they're cheap, stable, and easy to modify. They have many uses and can be made into unique structures. Cross-linkable epoxy resin is perfect for creating these new sorbents. Having multiple functional groups like amino, hydroxy, and ether in the network could help remove dyes more effectively [8]. Numerous techniques, such as extraction, micro-solid phase extraction, micro column preconcentration, UV semi-degradation, advanced oxidation, photocatalytic degradation–adsorption process, adsorption, and membrane filtration, have been proposed to treat industrial sewage in recent years. Each technique has pros and cons and removal efficiency [9-13]. The Fenton process is one of the best methods for eliminating organic contaminants since it is easy to use and maintain, has a high oxidation power, oxidizes quickly, and uses less energy when iron catalyst is present.

The research approach involves introducing various amine compounds units and utilizing polyfunctionality to promote adsorption within the network for the adsorptive removal of cationic Acridine Orange (AO) dye and comparing adsorption systems with the Fenton process.

2. Experimental

2.1. Material

Epoxy resin (Diglycidyl ether of bisphenol A) and commercial hardener polyamine were purchased from Kuwait Corporation Chemical Supplier in KUWAIT. 4-aminopyridine (CAS Number: 504-24-5), 3,3-diaminobenzidene (CAS Number: 7411-49-6) was obtained from RDH Chemical Company, Germany, and 4-aminobenzoyl hydrazine (CAS Number: 5351-17-7) and Acridine Orange (CAS Number: 65-61-2) dye from Sigma, Germany. Dimethyl formamide (CAS Number: 68-12-2) DMF from Fluka, Germany. Ethanol, Methanol and 1,4-dioxane from Alpha Chemika, India.. The dye has a molecular formula and weight of $C_{17}H_{19}N_3$ and 265.36 g·mol^{-1} respectively. The dye stock solutions were prepared in concentration (1000 mg L^{-1}) using double distilled water. The pH was adjusted through dilute solutions (0.1-0.01 mol L^{-1}) of NaOH and HCl from VWR. Fourier-transform infrared spectroscopy (FT-IR) was recorded on Shimadzu, FTIR-8400S spectrometer/Japan as KBr pellets, and Thermal Gravimetric Analysis (TGA) was also applied to determine the weight loss behavior of the epoxy resin with various amino compounds as curing agents.

The AO dye absorbance was measured at a wavelength of 492nm, using a UV-visible spectrophotometer (PG Instrument T80 + UV/VIS). The removal efficiency of dye was expressed as a percentage (%Removal Efficiency) for the Fenton approach, Equation1, while the amount of AO dye adsorbed per unit weight of the adsorbent at a specific time, q (mg g^{-1}), was determined through the utilization of Equation 2.

$$\%\ Removal\ Efficiency = \frac{C_0 - C_e}{C_e} \times 100 \quad \text{(Eq.1)}$$

$$q = \frac{(C_0 - C_e)V}{M} \quad \text{(Eq.2)}$$

Where, Ce and C_0 are references to the concentration at temperature (T) and initial concentration of AO dye in (mg) per (L), V represents the volume of the dye in (L), while M is the weight of the epoxy adsorbents in (g).

2.2. Preparation of Hardener Epoxy Resin

2.2.1.Preparation of cured Epoxy resin for 4-aminopyridine (E1)

A mixture of epoxy resin (2.6 g), 4-aminopyridine (1.34 g), 1,4-dioxane (4.8 mL), and methanol (2.4 mL) was refluxed at 95-100 °C for 3 hr. The cured product was purified by thoroughly washing with dioxane/methanol several times. Cured epoxy was collected and crushed as a particle for identification and characterization [14].

2.2.2.Preparation of cured Epoxy resin for both 3,3-diaminobenzidine (E2) and 4-aminobenzoyl hydrazine (E3)

Epoxy resin 5 mL (Diglycidyl ether of bisphenol A) dissolved in solvent 70 mL DMF. Then amino compounds (3,3-diaminobenzidene or 4-aminobenzoyl hydrazine) were added at 250 °C, the mixture was cast on the petri-dish uniformly. The petri-dish was dried in a hot air oven at 150-155 °C and left in a hot oven for 1 hr. The cured epoxy resin was taken out and washed with DMF several times. Then cured epoxy was crushed as a particle for identification and characterization [15-17].

2.2.3.Preparation of cured Epoxy resin for polyamine (E4)

Epoxy resin and polyamine (curing agent) were used in a 3:2 equivalent ratio (excess quantity of agent was used to ensure remaining free amino groups), mixed together until a homogeneous mixture was well blended. Next, the mixed system was washed with ethanol several times to remove trace unreacted polyamine, then poured into the metal mold and left in a hot air oven at 100°C for 4 h. Finally, the cured system was ground and collected for identification and characterization. Figure 1 represented prepared hardener epoxy compounds [18].

2.3. Degradation of Acridine Orange by Fenton Process

In this study, four variables: pH (2-12), contact time (2-20) minutes, dye concentration (100-1200 mg L^{-1}), and ratio of Fenton reagent (1:0.5 - 1:10) were considered. The four steps of this method were completed at room temperature: Initially, the ideal dye concentration investigated using a range of color concentrations at pH_{pzc}, a 5-minute contact period, and a 1:1 H_2O_2/Fe^{2+} ratio. Various dye concentrations (100, 200, 400, 600, 800, 1000 and 1200 mg L^{-1}) were created in this phase. Following this, the samples were centrifuged for five minutes. The filtrate was then moved to a spectrophotometer to determine the remaining dye concentration and the absorbance

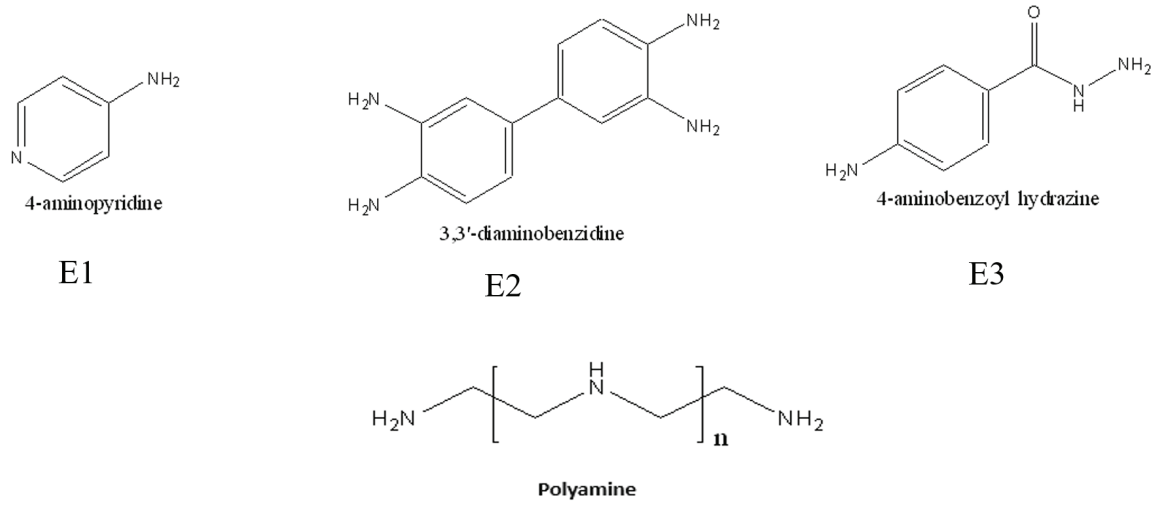

Fig. 1. Structures of prepared hardener epoxy E1-E4

measured at 492nm. Six different pH values (2, 4, 6, 8, 10 and 12) were studied in the second step to investigate the optimum pH. By fixing the optimum dye concentration (800 mg L^{-1} from the previous step), other variables, namely the reaction time (5 minutes) and the H_2O_2/Fe^{2+} ratio (1:1) were kept constant like the first step. In this step, the optimum pH was determined 4. The optimum H_2O_2/Fe^{2+} ratio determined by applying six deferent ratios (1:0.5, 1:1, 1:2, 1:4, 1:8, 1:10) under the optimum conditions, namely C_0=800 mg L^{-1}, pH 3, and 5 minutes of reaction time. After centrifugation for 5 minutes, method solutions were transferred to the spectrophotometer and the optimal ratio of 1:4 was obtained for H_2O_2/Fe^{2+}. In the last Fenton optimization step, the reaction time of Fenton degradation was studied at five different times (2, 5, 10, 15, 20 minutes).

2.4. Batch Adsorption Experiments

Batch adsorption experiments of AO dye were conducted to assess the adsorption parameters and factors influencing the adsorption. A 100mL solution (500.0 mg L^{-1} of AO dye) kept in contact with 100.0 mg of adsorbents E1, E2, E3 and E4 by a thermostat shaker at 25 °C and 245 rpm for a specific period (15–180 min). After the end of each agitation time, the epoxy resins were separated from the solution by simple filtration. The remaining amount of AO dye was determined by UV– visible spectroscopy at 492nm [19,20].

2.5. Characterization of Prepared Epoxy Resins

2.5.1.Fourier transform infrared spectroscopy (FTIR)

Based on Figure 2, the FTIR spectrum of epoxy resin (Neat) shows bands at 3402 cm^{-1} and 916 cm^{-1} wavenumber bands, which indicate the presence of (OH) and epoxy ring CH_2-O-CH. Also, band at 3049 cm^{-1} assigned to the -CH-(O-CH_2) epoxy, band at 1028 cm^{-1} to the -C-O-C- present in the structure. The vibration of C-O bonding of the hydroxyl group can be observed at 1028 cm^{-1}. For 4-Aminopyridine (E1) the bands observed at 3342, 3236, and 1658 cm^{-1} are attributed to the N–H asymmetric, symmetric, and in-plane deformation stretching vibration v, respectively. Band at 2923 cm^{-1} is assigned to the C-H aliphatic stretching. Band at 1603 cm^{-1} is related to the C=N stretching vibration of the pyridine ring. Two absorption bands at 1504 and 1456 cm^{-1} were observed, attributed to the C=C stretching vibration of the pyridine. The presence of the aminopyridine units was further substantiated with the appearance of C–N stretch band at 1384 cm^{-1} [21]. The FTIR study of cured epoxy resin with 3,3-diaminobenzidine (E2) of the cured epoxy resin shows broad band appearance at 3350 cm^{-1}, which is from N–H secondary amine and primary hydroxy group stretching vibration, also there were no band at 916 cm^{-1} (band due to epoxy groups) [22] as represented by Figure 3. The FT-IR spectrum of epoxy-4-aminobenzoyl hydrazine (E3) was shown in Figure 4. Due to conjugated effect between carbonyl and benzene, the carbonyl C=O absorb at lower frequency 1658 cm^{1} contribute to stretching vibration of benzoyl hydrazine. The absorption band at 1288 cm^{-1} was mixed, including C-N and N-H bending stretching vibration. The epoxy group (Oxirane ring) band 916 cm^{-1} was reduced [23]. For Polyamine (E4) the bands of the epoxy group at 3049 cm^{-1} and 916 cm^{-1} decrease during the curing process, as shown in the FTIR spectrum (Fig. 5). The bands for aliphatic -CH_2 bending and -CH_3 symmetrical and asymmetrical vibrations are observed between 2300-2400 cm^{1} for both the polyamine. Polyamine containing a distinct broad N–H stretching absorption around 3363 cm^{-1}, while the epoxy resin has a band at 3402 cm^{-1}, which belongs to hydroxyl stretching vibration. However, it is difficult to evaluate the band attributed to polyamine stretching vibration, due to the overlapping with the epoxy resin stretching bands. Like agents above, the curing was confirmed that the relative intensity of the oxirane ring band (916 cm^{-1}) disappeared [24].

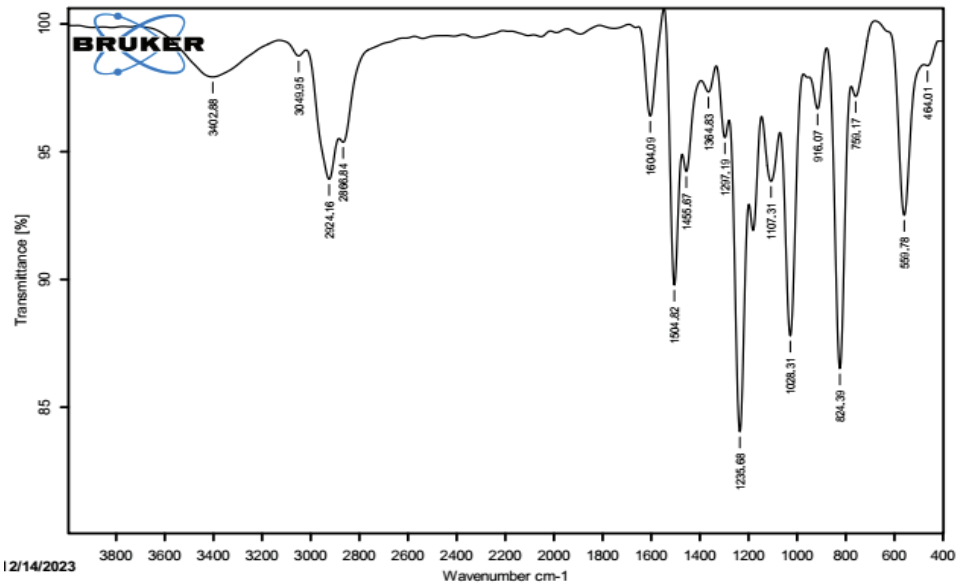

Fig. 2. FTIR spectra for 4-Aminopyridine (E1)

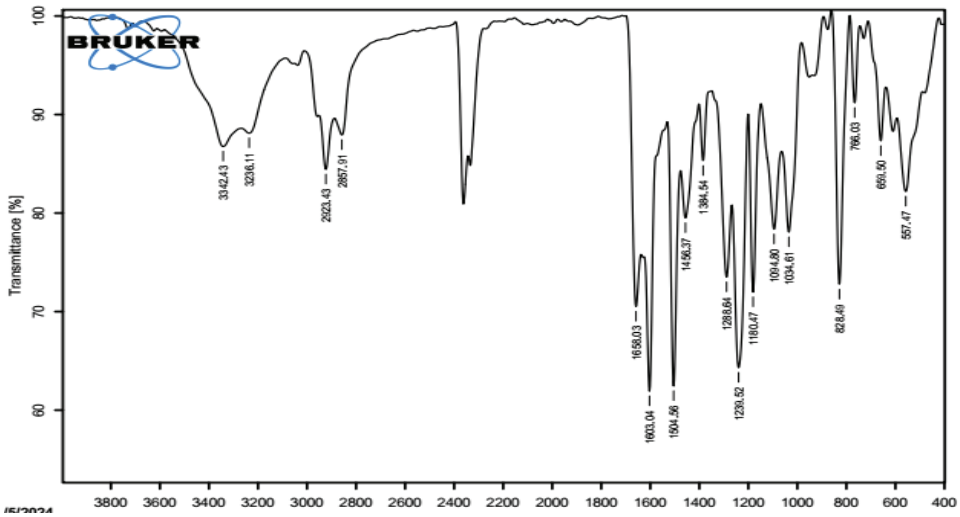

Fig. 3. FTIR spectra for 3,3-diaminobenzidine (E2)

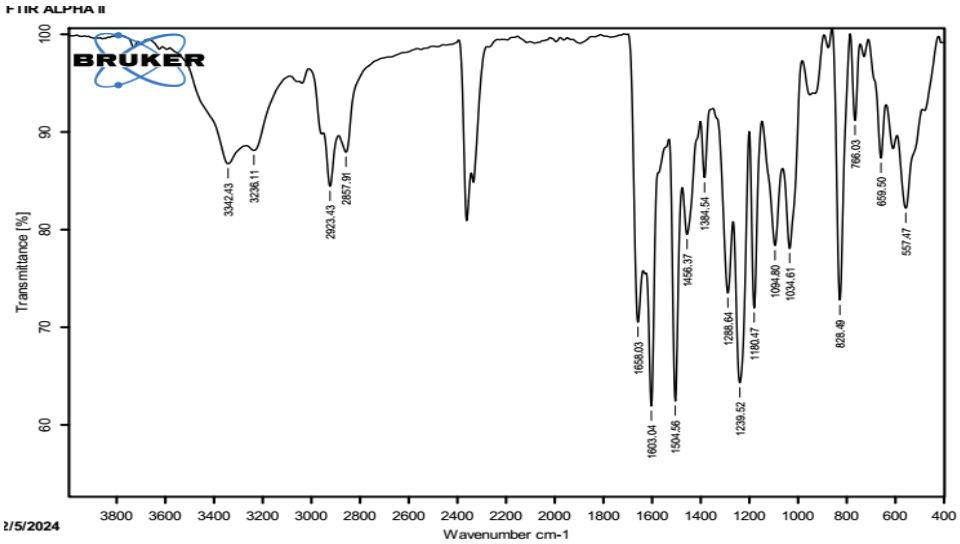

Fig. 4. FTIR spectra for 4-aminobenzoyl hydrazine (E3)

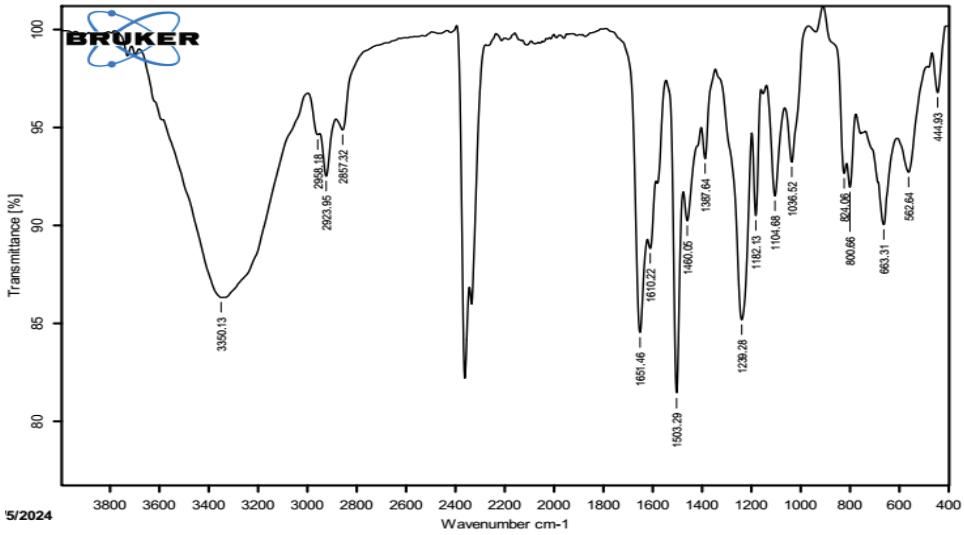

Fig. 5. FTIR spectra for polyamine (E4)

2.5.2. Thermogravimetric analysis (TGA)

A thermogravimetric analysis (TGA) was used to determine the epoxy resin's weight loss behavior with various amino compounds as curing agents. The degradation process was run at a maximum temperature of 550 °C in an inert atmosphere. The crosslinked resin's weight loss was calculated, and Table 1 displays the weight loss rates as a function of temperature. E1-E4 were thermally stable at 200 ◦C of EDAB and EAPy and 350 °C of EABH and EPAm. They decompose in a single step in the 215 to 360°C. Furthermore, it is evident from the curves analysis that the inclusion of aromatic rings improves thermal stability, especially true of EDAB, which develops char content around 20% after reaching the temperature above 550 °C. The products have a slight mass loss due to physically adsorbed water on the EABH surface, visible at temperatures between 98 and 100 °C. As shown in the results data listed in Table 1, thermal stability of resins occurred when the 3,3-diaminobenzidine reacted with epoxy resin due to diaromatic rings (char content 20%). Compared with curing epoxy resin by commercial polyamine hardener, which had a lower char content of 5%, this may have returned to the aliphatic nature of polyamine chemical structure.

Table 1. Thermal Gravimetric Analysis (TGA) of Epoxy systems

Epoxy Resin	UDT (°C)	WL%	TWL (°C)	RD (%/min)	CC% (550 °C)
E1	215	25	330	4.2	20
		50	365		
		75	490		
E2	235	25	340	4.31	7
		50	375		
		75	410		
E3	363	25	158	3.58	14
		50	390		
		75	460		
E4	360	25	360	10	5
		50	380		
		75	410		

UDT: Ultimate Decomposition Temperature °C
WL%: Weight Loss%
TWL: Temperature at Weight Loss °C
RD: Rate of Decomposition %/min
CC%: Char Content %

3. Results and Discussion

3.1. Degradation of AO dye by Fenton Process

3.1.1.Effect of Dye Concentration

Figure 6 illustrates the effect of dye concentration on the removal efficiency, when the dye concentration was between 100-400 mg L^{-1}, the removal percentage was obtained at 99.0-89.7%, respectively. However, when the dye concentration increased, the removal rate decreased; therefore, 800.0 mg L^{-1} dye solution was chosen as the initial dye concentration (C0), corresponding to about 60% removal. The concentration that corresponds to this ratio was chosen because it can be increased when examining the trade-off process for other factors like pH, the H_2O_2/Fe^{2+} ratio, and contact time. Such outcomes were likewise attained by Fahimeh Moghadam et.al. [25].

3.1.2.The Effect of pH in the Dye Removal

Studying the effect of pH value is an essential point in the Fenton process [26]. According to the results obtained, Figure 7 shows that the maximum dye removal efficiency was observed at pH 4, and the high removal efficiency was obtained in the low pH values (acidic). Iron ions were often insoluble under acidic media conditions, giving hydroxyl radicals a potent oxidizing ability. Acids contribute to hydrogen peroxide's stability. Studies show that pH values of 3 to 4 are optimal for Fenton tests because higher or lower pH values allow the ferrous (Fe^{3+}) ions to be liberated as sludge from the reaction media [26,27]. When pH exceeds 3, Fe^{3+} precipitates as $Fe(OH)_3$ and decomposes H_2O_2 into H_2O and O_2. In chemical processes, the concentration of iron ions is reduced by elevated pH levels [28]. On the other hand, ferric ion precipitation in the form of hydroxide can lead to high pH values. In this instance, iron converts H_2O_2 into H_2O and O_2 [29], and the oxidation rate of the oxidation process becomes less due to the decrease of hydroxyl radical [30].

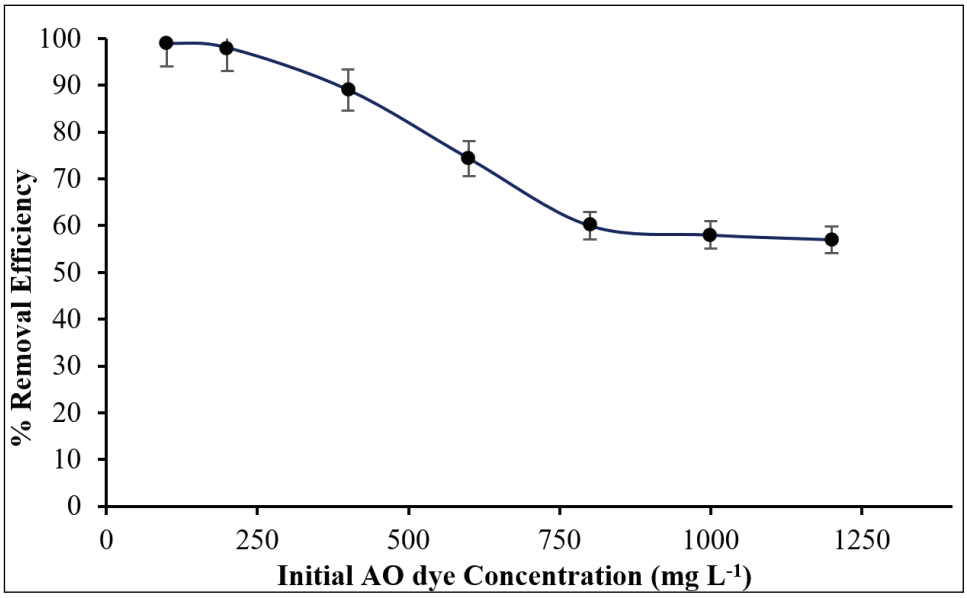

Fig. 6. Effect of AO dye initial concentration on removal efficiency

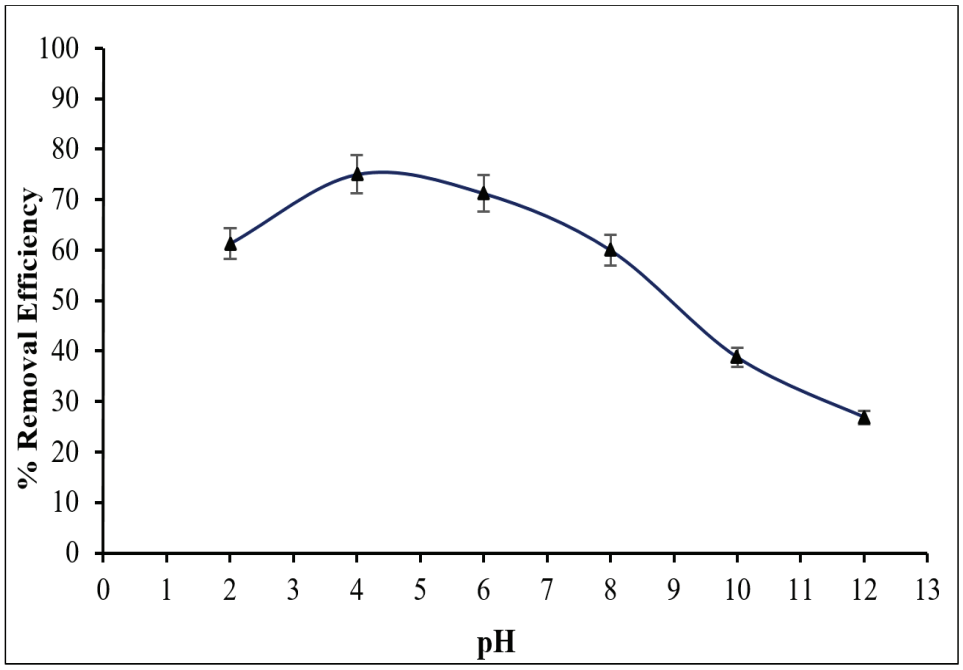

Fig. 7. Effect of dye solution pH value on removal efficiency

3.1.3.Effect of H_2O_2/ Fe^{2+} Ratio in the Dye Removal

The optimization study for ratio of H_2O_2/ Fe^{2+} in Figure 8, indicates that the maximum removal efficiency gets at ratio 1:4 and then decline in trend in the ratio of 1:8 to 1:10, this behavior is explained by the fact that H_2O_2 cannot oxidize AO dye in the absence of iron ions; instead, the presence of ferrous (Fe^{3+}) ions caused the (OH) radical to develop, which in turn triggered the oxidation process. Controlling the ferrous ion concentration in the Fenton reaction is crucial and highly influential since, in contrast, excessive H_2O_2/Fe^{2+} ratios exceeding 1:4 led to a decrease in the efficiency of dye degradation.

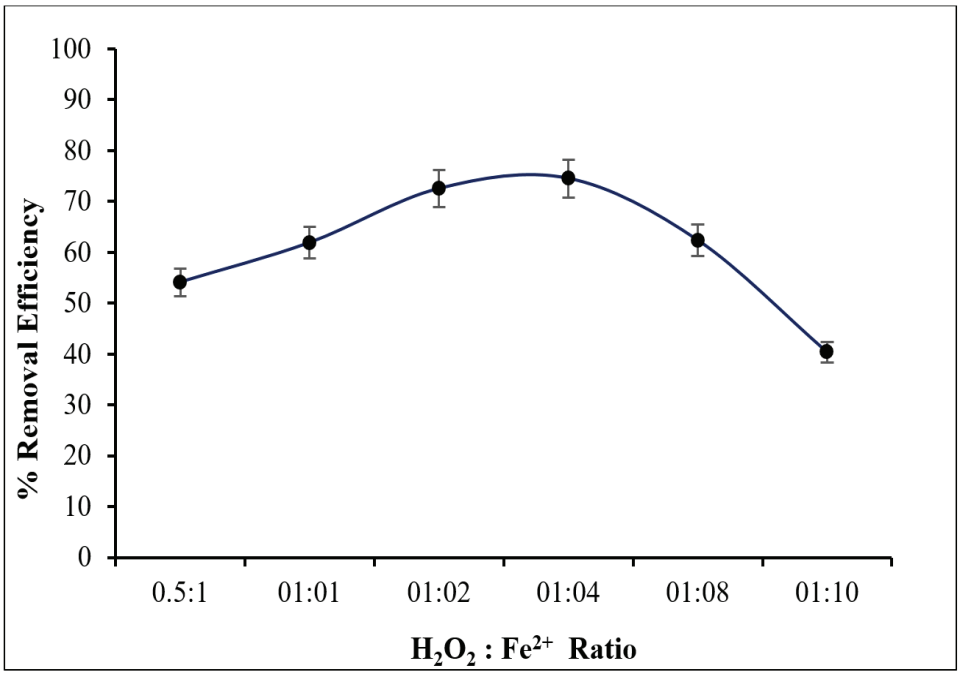

Fig. 8. Effect of H_2O_2/Fe^{2+} ratios on removal efficiency

3.1.4. The Effect of Time on the Dye Removal

The effect of time on AO dye removal efficiency was applied at optimal conditions obtained in previous experiments. The results showed that, when reaction times increased from 2 to 10 minutes, the removal efficiency first showed an ascending trend, but later on, because of intermediate compounds formation that reacted with (OH) radicals, quench potential and eliminate hydroxyl [31]. Within the initial few minutes of the Fenton reaction, a significant amount of hydroxyl free radicals are created [32,33]. However, the degree of color removal decreases significantly over time due to the generation of hydroxyl radicals [34]. The impact of reaction time on the elimination of AO dye is shown in Figure 9.

3.2. Adsorption of AO dye onto prepared Hardener Epoxy Resin

3.2.1. Effect of pH

For all adsorbents, the impact of pH on the adsorption capacities (qe) was investigated at an initial AO dye concentration of 500.0 mg L^{-1}. The pH influence of the adsorption capabilities at various pH values ranging from 2.0 to 12.0 at 25°C is shown in Figure 10.

The data indicates a notable increase in AO dye adsorption from 2.0 to 10.0 pH, with adsorption capacity remaining constant at 12 for adsorbents E1-E4. However, with the increasing pH values, this fact was also reported by other studies [33]. Adsorption of adsorbents tends to be favorable with rising pH values, because the electrostatic attraction between adsorbate species of cationic dyes (AO) increased.

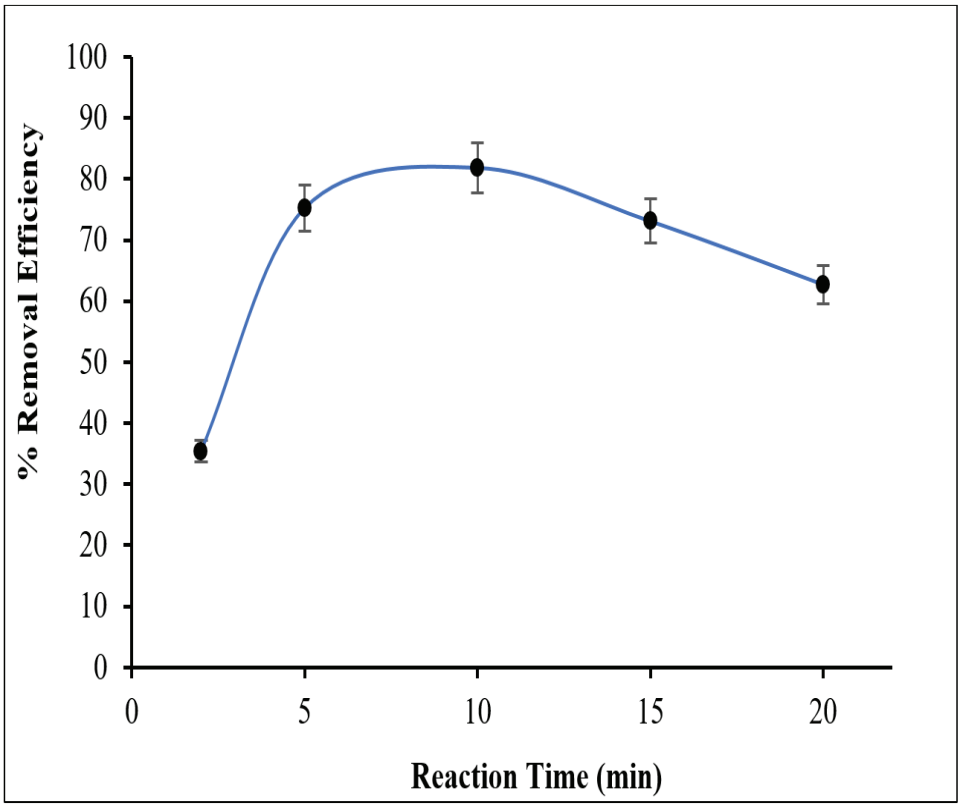

Fig. 9. Effect of reaction time on removal efficiency

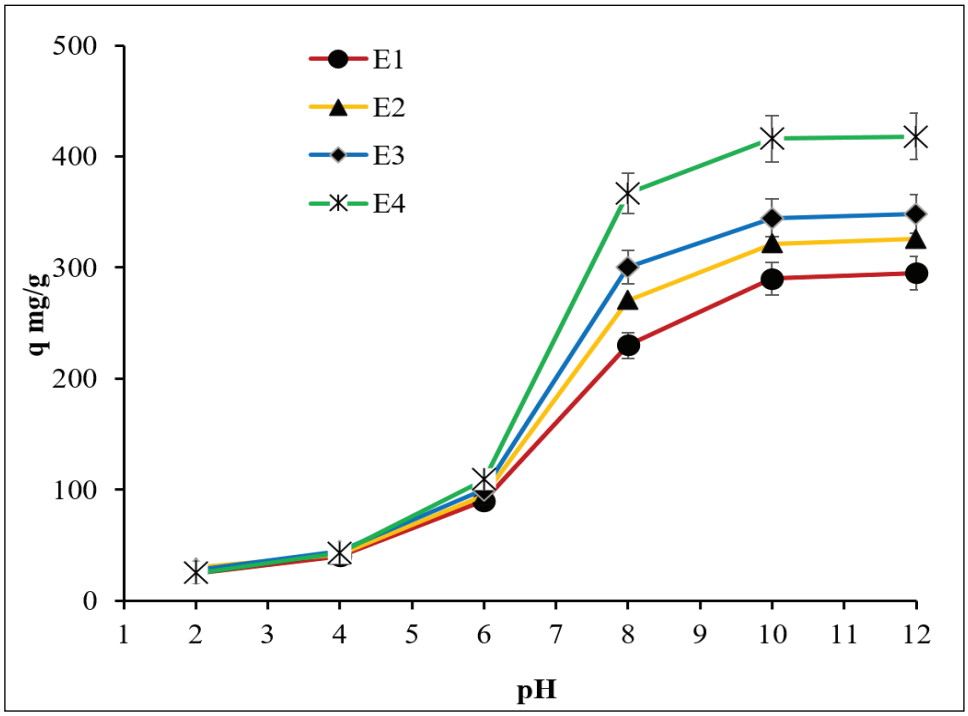

Fig. 10. Effect of dye solution pH value on adsorption capacity

3.2.2.Agitation time effect on the adsorption

Figure 11 shows the influence of shaking time on the adsorption of AO dye at pH 10.0 onto adsorbents E1-E4. The adsorption of AO increases sharply for a period of time (15–60 min), and then the trend reaches a steady state within a period of time (60–180 min) for all adsorbents.

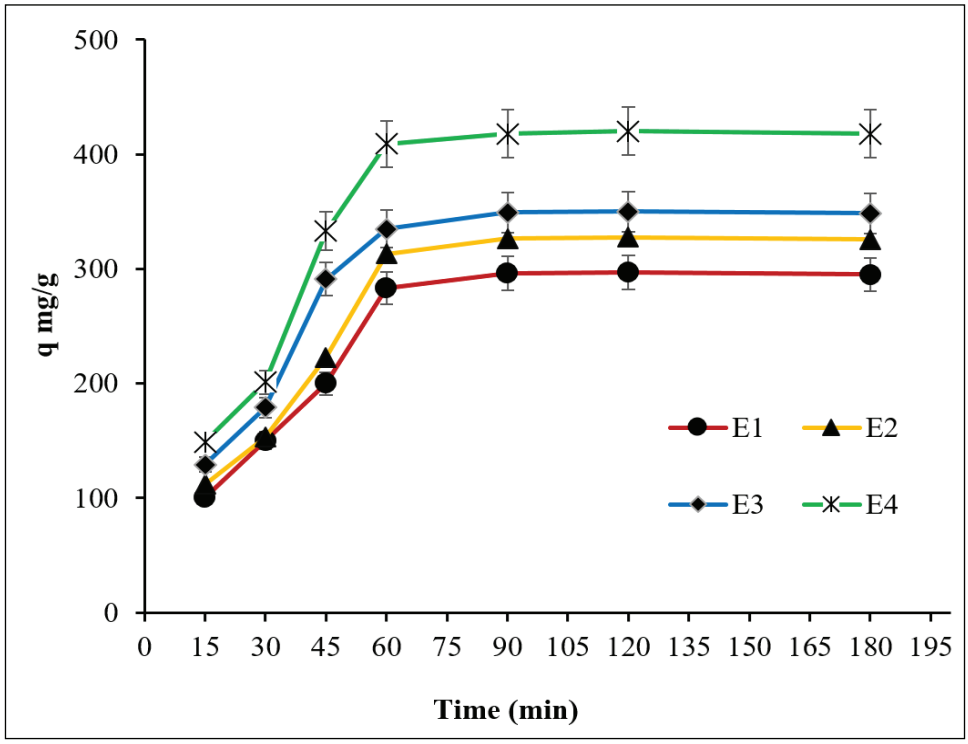

Fig. 11. Effect of agitation time on adsorption capacity

3.2.3.Adsorption Isotherm

The distribution of molecules between the liquid and solid phases at equilibrium is displayed by the adsorption isotherm. One of the most important steps in determining which model best describes the adsorption process is to analyze the isotherm data by plotting the data to various isotherm models [34]. The experimental data in this work are analyzed using the Langmuir and Freundlich models. The limitation of the Langmuir isotherm is the maximum adsorption that fits with the saturated monolayer of liquid (adsorbate) molecules on the solid (adsorbent) surface [35]. Figure 12 exhibits the plots of Langmuir adsorption isotherms. The linearized form of the Langmuir model is given in Equation 3.

$$\frac{C_e}{q_e} = \frac{1}{q_{max} + K_L} + \frac{C_e}{q_{max}} \quad \text{(Eq.3)}$$

The heterogeneous exponentially decaying distribution that underlies the Freundlich isotherm [35] fits the tail region of the heterogeneous distribution of adsorbed nicely. The empirical equation for a general Freundlich isotherm is as Equation 4.

$$lnq_e = lnK_F + {}^{1}/_{n}\, lnC_e \quad \text{(Eq.4)}$$

where K_F (L mg^{-1}) is a constant for the adsorption or distribution coefficient, and it reflects the adsorption capacity at equilibrium concentration, Freundlich adsorption isotherms represented in Figure 13, Table 2 displays results obtained from the isotherm study.

Table 2. Langmuir and Freundlich Isotherm Parameters for Adsorption of AO dye onto E1-E4 at 25°C.

Adsorbents	Langmuir			Freundlich		
	q_{max}	K_L	R^2	K_F	n	R^2
E1	980.39	0.0019	0.9989	15.376	1.8228	0.9883
E2	1515.2	0.0014	0.9969	10.305	1.5221	0.9944
E3	1694.9	0.0015	0.9918	11.353	1.4921	0.9879
E4	1851.9	0.0029	0.9898	25.237	1.6255	0.9927

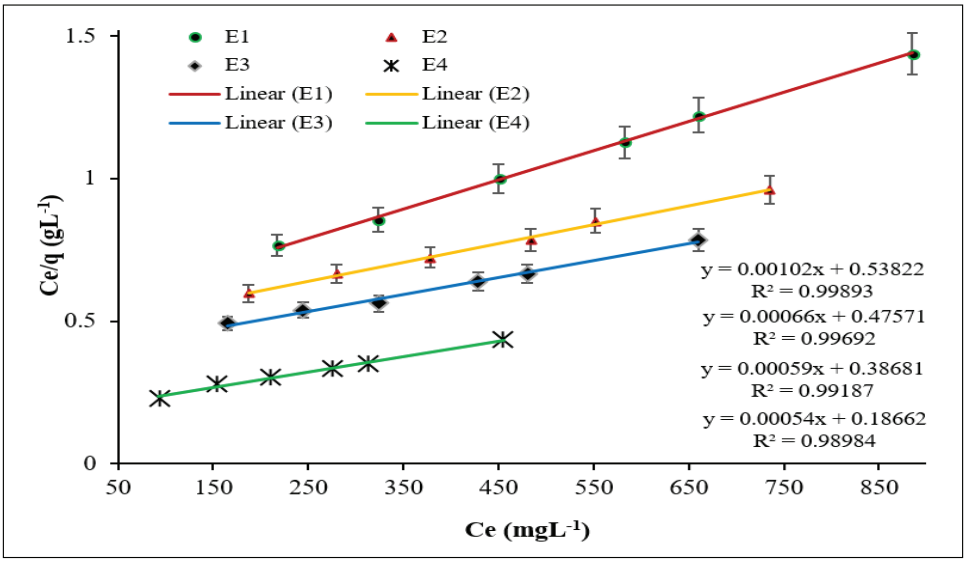

Fig. 12. Langmuir model adsorption isotherms for AO dye onto E1-E4

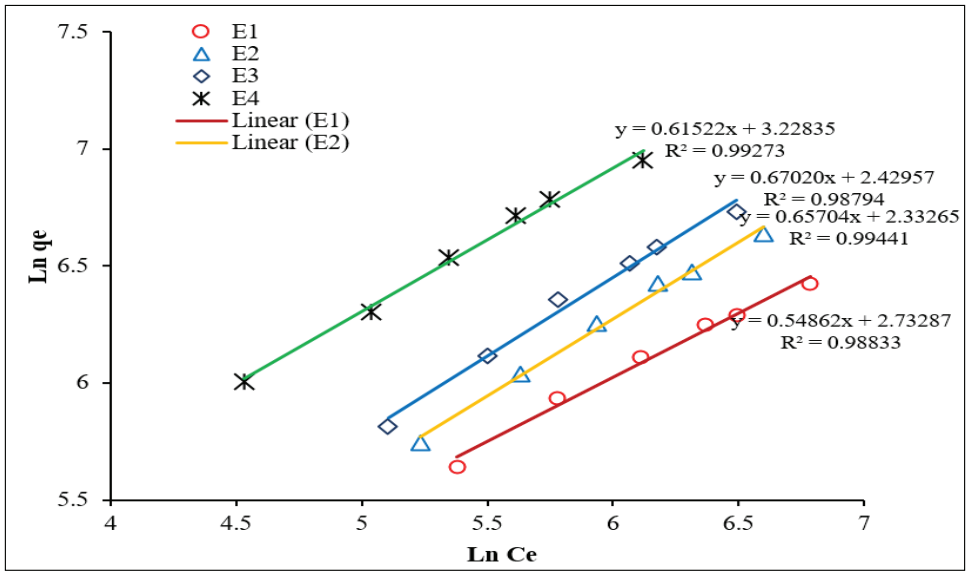

Fig. 13. Freundlich model adsorption isotherms for AO dye onto E1-E4

3.3. Performance Evaluation

The maximum adsorption capacity of AO dye has been compared with the literature values of other adsorbents and listed in Table 3. All of the methods used for AO have considerably higher max values than the adsorption onto thermosetting epoxy resin E1-E4 used in this study.

4. Conclusion

This study employed adsorption and Fenton methods for removal of cationic AO dye, the efficient removal from aqueous solutions by using the new hardener epoxy resins E1-E4 as adsorbents. The maximum adsorption of AO was obtained at pH 10. From closed R^2 values to one of the

Table 3. Summary of AO adsorption capacities of various adsorbents

Type of adsorbent	q_{max} , (mg g^{-1})	Reference
BG/GO; IL-MWCNTs; CQDs	200-350	[36-38]
sugar beet pulp	324.85	[39]
Gt/Cu-AC np	95.43	[40]
MGA-PP-RFHN	202.63	[41]
dry biomass of Bacillus cereus	210.46	[42]
Watermelon rinds	69.44	[43]
E1	980.39	This Study
E2	1515.2	This Study
E3	1694.9	This Study
E4	1851.9	This Study

BG/GO; IL-MWCNTs; CQDs: Bismuth oxide coupled to heterogeneous graphene/graphene oxide; Ionic liquid coated on MWCNTs; Carbon Quantum Dots
Gt/Cu-AC np: Green tea/copper-activated carbon nanoparticles
MGA-PP-RFHN: Mesoporous glutamic acid-g-polyacrylamide/plaster of paris/riboflavin hydrogel nanocomposite

Langmuir model plots for all adsorption systems, we concluded the chemosorption mechanism. From the calculation of the Langmuir equation (qmax), values for E1-E4 were 980.39, 1515.2, 1694, and 1851.9 mg g^{-1} respectively. On the other hand, the optimum parameters of the Fenton process were investigated: pH =3, H_2O_2/Fe^{2+} ratio of 1:4, contact time = 10 minutes, and the dye concentration of 800mg.L^{-1} was obtained. In addition, the results showed that the initial dye concentration influenced the concentration of hydrogen peroxide and iron sulfate. The percentage of Acridine Orange removal was 81.87%, and the results of this study showed that the Fenton process was a practical approach to remove AO dye from its solution.

5. Acknowledgements

The authors thank the University of Basra, Al-Ashar–Corniche Street, Basra, Iraq.

6. References

[1] M. S. Tsuboy, J. P. F. Angeli, M.S. Mantovani, S. Knasmuller, G.A. Umbuzeiro, L.R. Ribeiro, Genotoxic, mutagenic and cytotoxic effects of the commercial dye CI Disperse Blue 291 in the human hepatic cell line HepG2, Toxicol. In Vitro, 21 (2007) 1650–1655. https://doi.org/10.1016/j.tiv.2007.06.020

[2] S. Sultana, M.D. Khan, S. Sabir, K.M. Gani, M. Oves, M.Z. Khan, Bio-electro degradation of azo-dye in a combined anaerobic–aerobic process along with energy recovery, New J. Chem., 39 (2015) 9461–9470. https://doi.org/10.1039/C5NJ01610J

[3] C. Zhang, P.C. Zhu, L. Tan, J.M. Liu, B.E. Tan, X.L. Yang, H.B. Xu, Triptycene-based hyper-cross-linked polymer sponge for gas storage and water treatment, Macromol., 48 (2015) 8509–8514. https://doi.org/10.1021/acs.macromol.5b02222

[4] N.R. Paluvai, S. Mohanty, S.K. Nayak, Synthesis and modifications of epoxy resins and their composites: A review, Plast. Technol. Eng., 53 (2014) 1723–1758. https://doi.org/10.1080/03602559.2014.919658

[5] J. Xu, J. Yang, X. Liu, H. Wang, J. Zhang, S. Fu, Preparation and characterization of fast-curing powder epoxy adhesive at middle temperature, Royal Soc. Open Sci., 5 (2018) 180566. https://doi.org/10.1098/rsos.180566

[6] P.S. Beata, W. Monika, K. Łukasz, Synthesis, characterization and sorption ability of epoxy resin-based sorbents with amine groups, Polymers, 13 (2021) 4139. https://doi.org/10.3390/polym13234139

[7] G. Samaresh, A. Mridula, Removal of azo dye molecules from aqueous solution using novolac resin based network polymer, Bull. Chem. Soc. Japan, 84 (2011) 349–351. https://doi.org/10.1246/bcsj.20100245

[8] M. M. Asl, F. Atabi, Functionalized graphene oxide with bismuth and titanium oxide nanoparticles for efficiently removing formaldehyde from the air by photocatalytic degradation–adsorption process, J. Anal. Test., 7 (2023) 444-458. https://doi.org/10.1007/s41664-023-00272-0

[9] S. Teimoori, A. H. Hassani, M. Panahi, N. Mansouri, An immobilization of aminopropyl trimethoxysilane-phenanthrene carbaldehyde on graphene oxide for toluene extraction and separation in water samples, Chemosphere, 316 (2023) 137800. https://doi.org/10.1016/j.chemosphere.2023.137800

[10] S. Teimoori, Rapid extraction of BTEX in water and milk samples based on functionalized MWCNTs by dispersive homogenized-micro-solid phase extraction, Food Chem., 421 (2023) 136229. https://doi.org/10.1016/j.foodchem.2023.136229

[11] S. Teimoori, A. H. Hassani, New extraction of toluene from water samples based on nano-carbon structure before determination by gas chromatography, Int. J. Environ. Sci. Technol., 20 (2023) 6589–6608. https://doi.org/10.1007/s13762-023-04906-9

[12] F. Golbabaei, On-line micro column preconcentration system based on amino bimodal mesoporous silica nanoparticles as a novel adsorbent for removal and speciation of

chromium (III, VI) in environmental samples, J. Environ. Health Sci.Eng., 13 (2015) 47. https://doi.org/10.1186/s40201-015-0205-z

[13] M. Asl, N. Mansouri, S. A. R. Haji Seyed Mirzahosseini, F. Atabi, Simultaneity comparative evaluation of toluene removal from the air by adsorption and UV semi-degradation-based adsorption procedure, Int. J. Environ. Sci. Technol., 21 (2024) 6677-6694. https://doi.org/10.1007/s13762-024-05503-0

[14] S. Ghosh, M. Acharyya, Pyridine-Rich Novolac-Based Network as an Effective Adsorbent for Removing Azo Dyes, Chem. Select, 5 (2020) 10727-10735 https://doi.org/10.1002/slct.202002024

[15] L. Feng, Y. Wang, Y. Wang, H. Liu, Study on reaction kinetics of epoxy resin cured by a modified dicyandiamide, J. Appl. Polym. Sci., 127 (2013) 1895-1900. https://doi.org/10.1002/app.37917

[16] P. Ranpara, P.N. Bhalerao, Curing of epoxy resin by using commercial amine/hydrazine and its effect on ultra violet spectrum advances in chemical, bio and environmental engineering, Conference paper, Environ. Sci. Eng., (2022) 949–956. http://dx.doi.org/10.1007/978-3-030-96554-9_63

[17] S. Yu, X. Li, M. Zou, X. Guo, H. Ma, S. Wang, Effect of the aromatic amine curing agent structure on properties of epoxy resin-based syntactic foams, ACS Omega, 5 (2020) 23268–23275. https://doi.org/10.1021/acsomega.0c03085

[18] H. Yamasaki, S. Morita, Epoxy curing reaction studied by using two-dimensional correlation infrared and near-infrared spectroscopy, J. Appl. Polymer Sci., 119 (2011) 871–881. https://doi.org/10.1002/app.32787

[19] H.S. Al-Niaeem, Thermal stability of some new metal containing polymers based on resol- bisphenol A formaldehyde resin, Res. J. Sci. Technol., 7 (2015) 2349-2988. https://doi.org/10.5958/2349-2988.2015.00025.X

[20] A.A. Abdulwahid, A.A. Alwattar, A. Haddad, M. Alshareef, J. Moore, G. Y. Yeatesb, P. Quayleb, An efficient reusable perylene hydrogel for removing some toxic dyes from contaminated water, Polymer Int., 70 (2021) 1234–1245. http://dx.doi.org/10.1002/pi.6186

[21] Y. Chen, Y. Ma, Q. He, Q. Qiuxia Han, Construction of pyridinium/*N*-chloramine polysiloxane on cellulose for synergistic biocidal application, Cellulose**,** 26 (2019) 5033–5049. https://doi.org/10.1007/s10570-019-02437-6

[22] E. Ulker, M. Kavanoz, Synthesis of poly (Vinylferrocene) perchlorate/poly(3,3'-diaminobenzidine) modified electrode in dichloromethane for electroanalysis of hydroquinone, J. Braz. Chem. Soc., 26 (2015) 1947-1955. http://dx.doi.org/10.5935/0103-5053.20150173

[23] M. R. Rezaei Kahkhaa, A. Faghihi Zarandi, A review in analytical methods: Removal and extraction of pollutants in different matrixes by nanotechnology, Anal. Methods Environ. Chem. J., 7 (2024) 51-82. https://doi.org/10.24200/amecj.v7.i03.1004

[24] M. González González, J. Carlos Cabanelas, J. Baselga, Applications of FTIR on epoxy resins - identification, monitoring the curing process, phase separation and water uptake, materials science, engineering and technology, Intech Open Publisher Book, 2012. https://doi.org/10.5772/36323

[25] F. Moghadam, N. N. Kohbanan, Removal of reactive blue 19 dye using Fenton from aqueous solution, Avicenna J. Environ. Health Eng., 5 (2018) 50-55. https://doi.org/10.15171/ajehe.2018.07

[26] H. Lee, M. Shoda, Removal of COD and color from livestock wastewater by the Fenton method, J. Hazard. Mater., 153 (2008) 1314-1319. https://doi.org/10.1016/j.jhazmat.2007.09.097

[27] S. Meric, D. Kaptan, T. Olmez, Color and COD removal from wastewater containing Reactive Black 5 using Fenton's oxidation process, Chemosphere., 54 (2004) 435-441. https://doi.org/10.1016/j.chemosphere.2003.08.010

[28] P. Bautista, A.F. Mohedano, J.A. Casas, An overview of the application of Fenton oxidation to industrial wastewaters treatment, J. Chem. Technol. Biotechnol., 83 (2008) 1323-1338. https://doi.org/10.1002/jctb.1988

[29] L. Szpyrkowicz, C. Juzzolino, S.N. Kaul, A Comparative study on oxidation of disperse dyes by electrochemical process, ozone, hypochlorite and fenton reagent, Water Res., 35 (2001) 2129- 2136. https://doi.org/10.1016/S0043-1354(00)00487-5

[30] B.H. Hameed, T.W. Lee, Degradation of malachite green in aqueous solution by Fenton process, J. Hazard. Mater., 164 (2009) 468-472. https://doi.org/10.1016/j.jhazmat.2008.08.018

[31] P.V. Nidheesh, R. Gandhimathi, Electro Fenton oxidation for teh removal of Rhodamine B from aqueous solution in a bubble column reactor under continuous mode, Desalin. Water Treat., 55 (2015) 263-271. https://doi.org/10.1080/19443994.2014.913266

[32] A.A. Zorpas, C.N. Costa, Combination of Fenton oxidation and composting for the treatment of the olive solid residue and the olive mile wastewater from the olive oil industry in Cyprus, Bioresour. Technol., 101 (2010) 7984-7987. https://doi.org/10.1016/j.biortech.2010.05.030

[33] Y. Yang, P. Wang, S. Shi, Y. Liu, Microwave enhanced Fenton-like process for the treatment of high concentration pharmaceutical wastewater, J. Hazard. Mater.,168 (2009) 238-245. https://doi.org/10.1016/j.jhazmat.2009.02.038

[34] A.A. Albaheli, PhD Thesis(chemist), Basrah university, Basrah, 2020. https://www.researchgate.net/profile/Alaa_Mizhir

[35] S.M. Saleh, PhD Thesis(chemist), Basrah university, Basrah, 2024. https://doi.org/10.13140/RG.2.2.19385.42086

[36] A. Faghihi-Zarandi, J. Rakhtshah, B. B. Yarahmadi, A rapid removal of xylene vapor from environmental air based on bismuth oxide coupled to heterogeneous graphene/graphene oxide by UV photo-catalectic degradation-adsorption procedure, J. Environ. Chem. Eng., 8 (2020) 104193. https://doi.org/10.1016/j.jece.2020.104193

[37] R. Ashouri, N. Mansouri, Dynamic and static removal of benzene from air based on task-specific ionic liquid coated on MWCNTs by sorbent tube-headspace solid-phase extraction procedure, Int. J. Environ. Sci. Technol., 18 (2021) 2377-2390. https://doi.org/10.1007/s13762-020-02995-4

[38] R. Ashouri, S. A. Hajiseyed Mirzahosseini, N. Mansouri, Synthesis of carbon quantum dots from olive stones for efficient adsorption of benzene from the ambient air, J. Nanostruct., 11 (2021) 480-497. https://doi.org/10.22052/JNS.2021.03.007

[39] V. M. Vučurović, V. S. Puškaš, U. D. Miljić, Removal of acridine orange dye from aqueous solution by adsorption onto dried sugar beet pulp, Acta Periodica Technologica, 48 (2017) 307-314. https://doi.org/10.2298/APT1748307V

[40] K. Chandrika, A. Chaudhary, T. Mareedu, Adsorptive removal of acridine orange dye by green tea/copper-activated carbon nanoparticles (Gt/Cu-AC np), Mater. Today: Proceedings, 44 (2021) 2283–2289. https://doi.org/10.1016/j.matpr.2020.12.391

[41] N. Abbasi, S. A. Khan, T. Alam Khan, Statistical evaluation of liquid phase sequestration of acridine orange and Cr6+ by novel mesoporous glutamic acid-g-polyacrylamide/plaster of paris/riboflavin hydrogel nanocomposite, Environ. Res., 213 (2022) 113712. https://doi.org/10.1016/j.envres.2022.113712

[42] S. Bag, M.I. Hasan, D Halder, Biosorption of organic dye Acridine orange from aqueous solution using dry biomass of Bacillus cereus M116, Arch. Microbiol., 203 (2021) 3811-3823. https://doi.org/10.1007/s00203-021-02355-x

[43] S. Ahmed, S.H. Siham, A. Nuri, E.A. Marwa, Watermelon rinds as cost-efficient adsorbent for acridine orange: a response surface methodological approach, Environ. Sci. Pollut. Res., 30 (2023) 71554-71573. https://doi.org/10.1007/s11356-021-13652-9